

Hydrostatic equilibrium of causally consistent and dynamically stable neutron star models

P. S. Negi^{1*}

¹ *Department of Physics, Kumaun University, Nainital - 263 002, India*

Accepted — . Received — ;

ABSTRACT

We show that the mass-radius ($M - R$) relation corresponding to the stiffest equation of state (EOS) does not provide the necessary and sufficient condition of dynamical stability for the equilibrium configurations, since such configurations can not satisfy the ‘compatibility criterion’. In this connection, we construct sequences composed of core-envelope models such that, like the stiffest EOS, each member of these sequences satisfy the extreme case of causality condition, $v = c = 1$, at the centre. We, thereafter, show that the $M - R$ relation corresponding to the said core-envelope model sequences can provide the necessary and sufficient condition of dynamical stability only when the ‘compatibility criterion’ for these sequences is ‘appropriately’ satisfied. However, the fulfillment of ‘compatibility criterion’ can remain satisfied even when the $M - R$ relation does not provide the necessary and sufficient condition of dynamical stability for the equilibrium configurations. In continuation to the results of previous study, these results explicitly show that the ‘compatibility criterion’ *independently* provides, in general, the *necessary* and *sufficient* condition of hydrostatic equilibrium for any regular sequence. Beside its fundamental feature, this study can also explain simultaneously, both (the higher as well as lower) values of the glitch healing parameter observed for the Crab and the Vela-like pulsars respectively, on the basis of starquake model of glitch generation.

Key words: static spherical structures - dense matter - equation of state - stars: neutron - pulsars: individual: Crab: Vela.

1 INTRODUCTION

Characteristics of the super-dense objects like neutron stars (NSs) are based on the calculations of the EOS for the matter at very high densities. However, the nuclear interactions beyond the density of $\sim 10^{14} \text{g cm}^{-3}$ are empirically not well known (Dolan 1992) and the all known EOSs are only extrapolations of the empirical results far beyond this density range. In this regard, various EOSs based on theoretical manipulations are available in the literature (Arnett & Bowers 1977). Since the status of EOS of nuclear matter cannot be established empirically beyond a certain density range, one can apply physical constraints to obtain an upper bound of neutron star mass. Brecher and Caporaso (1976) assumed that the speed of sound in the nuclear matter equals the speed of light and obtained a value of $4.8M_{\odot}$ as an upper limit of the neutron star masses. However, the matter described by this stiffest EOS, $(dP/dE) = 1$ (geometrized units) or $P = (E - E_s)$ [where P is the pressure, E is the

energy-density and $E_s = 2 \times 10^{14} \text{g cm}^{-3}$ represents the surface density] has a super-dense self-bound state at the surface of the configuration where the pressure is vanishingly small, which represent the ‘abnormal state of matter’ (Lee 1975; Haensel & Zdunik 1989). This ‘abnormality’ may be specified as - (i) the pressure vanishes at the average nuclear densities, and (ii) the speed of sound is equal to that of light even when the pressure is vanishing small. This ‘abnormality’ can be removed if we ensure continuity of pressure, density and both of the metric parameters at the boundary of the structure (Negi & Durgapal 2000).

Earlier, Rhoades and Ruffini (1974), without going into the details of the nuclear interactions, assumed that beyond a certain density $4.6 \times 10^{14} \text{g cm}^{-3}$ (the range of densities where no extrapolated EOS is known) the EOS in the core is given by the criterion that the speed of sound attains the speed of light, that is, $(dP/dE) = 1$, and matched the core to an envelope with the BPS (Baym, Pethick & Sutherland 1971) EOS and obtained an upper limit for the neutron star mass as $3.2M_{\odot}$. Hartle (1978) emphasized that the maximum masses of neutron stars obtained in this manner in-

* E-mail: negi@aries.ernet.in; psnegi_nainital@yahoo.com

volve a scale factor, $k = [E_m/10^{14} \text{g cm}^{-3}]^{-1/2}$, such that, the matching density, E_m , plays a sensitive role to obtain an upper bound on neutron star masses. Usually, k is taken to be equal to or greater than one in all the conventional models. For the densities less than E_m , the matter composing the object is assumed to be known and unique. That is, the EOS of the envelope of these stars are chosen so that the ‘abnormalities’ in the sense mentioned above are removed. Friedman and Ipser (1987) calculated the masses of the neutron stars for different values of the matching densities using EOS given by BPS and NV (Negele & Vautherin 1973), respectively, and concluded that the EOS chosen for the envelope does not make any significant difference in the results, because in each case the mass in the envelope turns out to be insignificant as compared to that of the core containing the most stiff material.

In order to implement this ‘insignificant’ mass of the envelope component, Crawford & Demiański (2003) have recently constructed the NS models for seven representative EOSs of dense nuclear matter by covering a range of NS masses. They have computed the ‘fractional moment of inertia’ of the core component which is defined as the glitch healing parameter, Q , in the starquake mechanism of glitch generation as

$$Q = \frac{I_{\text{core}}}{I_{\text{total}}}, \quad (1)$$

where I_{total} represents the moment of inertia of the entire configuration. Their study shows that the much larger values of $Q (\geq 0.7)$ for the Crab pulsar are fulfilled by all but the six EOSs considered in the study corresponding to a ‘realistic’ neutron star mass range $1.4 \pm 0.2 M_{\odot}$. On the other hand, for the much lower values of $Q (\leq 0.2)$ corresponding to the case of the Vela pulsar, their models predict a NS mass $\leq 0.5 M_{\odot}$ which is too low as compared to the ‘realistic’ NS mass range. Thus, their study concludes the ‘starquake’ as a feasible mechanism for glitch generation in the Crab-like pulsars (corresponding to a larger value of Q) and the ‘vortex unpinning’, the another mechanism of glitch generation, suitable for the Vela-like pulsars (corresponding to a lower values of Q). However, it seems quite surprising that if the internal structure of NSs is supposed to be described by the same two-component conventional model, then why different kinds of glitch mechanisms are required to explain a glitch!

This is the purpose of this study to provide an insight about a fundamental ‘theorem’ concerning the hydrostatic equilibrium of NS models (which was lacking in the earlier studies) and to show that as soon as this theorem is implemented to an appropriate conventional NS sequence, the various shortcomings of the conventional NS models (as mentioned above) can be resolved.

2 REMOVAL OF ABNORMALITIES FROM THE STIFFEST EOS AND BOUNDARY CONDITIONS FOR NEUTRON STAR MODELS COMPATIBLE WITH HYDROSTATIC EQUILIBRIUM

In order to construct such an appropriate sequence of NS models, consistent with causality and dynamical stability,

we offer here an entirely different approach to the whole problem which will not only remove the ‘abnormalities’ of the stiffest EOS (as discussed earlier in detail under section 1) but can also assure the *necessary and sufficient* condition of hydrostatic equilibrium for the resulting configuration. Since, as we would show later in section 3 that the $M - R$ relations corresponding to the configurations (i) governed by the pure stiffest EOS, and (ii) those resulting from the removal of ‘abnormalities’ from the stiffest EOS (core-envelope models), do not provide the necessary and sufficient condition of dynamical stability unless the ‘compatibility criterion’ (Negi & Durgapal 2001) which states that: “for each and every assigned value of $\sigma [\equiv (P_0/E_0) \equiv$ the ratio of central pressure to central energy-density], the compactness ratio $u (\equiv M/R)$ of the entire configuration should not exceed the compactness ratio, u_h , of the corresponding homogeneous density sphere (that is, $u \leq u_h$)” is ‘appropriately’ satisfied by such configurations.

The present approach is based on the ‘theorem’ applicable to a wide range of conventional NS sequences (including the core-envelope models) provided that every member of such sequences satisfies the condition $(dP/dE)_0 = 1$ (here and elsewhere in the paper, the subscript ‘0’ represents the value of the corresponding quantity at the centre of the configuration). This theorem asserts that in order to assure the necessary and sufficient condition of dynamical stability for the mass, the maximum stable value of u (corresponding to the case of first maxima among masses in the mass-radius ($M - R$) relation) and the corresponding central value of ‘local’ adiabatic index $(\Gamma_1)_0 (\equiv [(P_0 + E_0)/P_0](dP/dE)_0)$ of such sequences must satisfy the inequalities, $u_{\text{max}} \leq u_{\text{max,abs}} \cong 0.3406$ and $(\Gamma_1)_0 \leq (\Gamma_1)_{0,\text{max,abs}} \cong 2.5946$ respectively (Negi 2007). In addition to the result of previous study regarding the ‘compatibility criterion’, we would show in the present study that “the $M - R$ relation (or the mass-central density relation) corresponding to an equilibrium sequence provides the necessary and sufficient condition of dynamical stability only when the ‘compatibility criterion’ for the equilibrium sequence is also satisfied. But the fulfillment of the ‘compatibility criterion’ does not depend upon the fulfillment of the necessary and sufficient condition of dynamical stability provided by the $M - R$ relation”. The proof of this statement would explicitly show that the fulfillment of ‘compatibility criterion’ independently provides, in general, the necessary and sufficient condition of hydrostatic equilibrium for any sequence composed of regular configurations, since the first sentence of this statement has already been proved in the previous study for the equilibrium sequences of the type mentioned above (Negi 2007).

In order to provide a proof of the last statement, the present paper deals with the construction of a four step consecutive study in the following manner

Step (1): We would construct the NS models corresponding to the pure stiffest EOS, $dP/dE = 1$, and show that the $M - R$ relation corresponding to this sequence does not provide the necessary and sufficient condition of dynamical stability, since the ‘compatibility criterion’ can not be fulfilled by the equilibrium configurations corresponding to this ‘abnormal’ EOS.

Step (2): We would construct the NS sequences composed of core-envelope models by considering the stiffest EOS, $dP/dE = 1$, in the core and the EOS of classical

polytrope, $d \ln P / d \ln \rho = \Gamma_1$ (where ρ is the density of the rest-mass and Γ_1 is the constant adiabatic index; see, e.g. Tooper 1965), in the envelope (so that each member of these sequences satisfy the extreme case of causality condition, $v = c = 1$, at the centre) for an ‘arbitrarily’ assigned value of pressure to density ratio, $(P_b/E_b) = (P_b/E_b)_1$ (say), at the core-envelope boundary. Though this procedure removes the ‘abnormalities’ from the stiffest EOS, but as we would show later in sec.3 that the $M - R$ relation corresponding to the NS models with an envelope $\Gamma_1 = 5/3$ and 2, do not provide the necessary and sufficient condition of dynamical stability, since the ‘compatibility criterion’ remains unsatisfied by various stable (as well as unstable) models corresponding to the said sequences.

Step (3): In this sub-section we would re-construct the NS sequence composed of core-envelope models as described in step (2) for the same boundary value of $(P_b/E_b)_1$. But instead of the constant $\Gamma_1 = 5/3$ and 2, the constant $\Gamma_1 = 4/3$ would be used for the envelope. We would show that although the ‘compatibility criterion’ is satisfied by all stable (as well as unstable) models comprising the sequence but still, the $M - R$ relation does not provide the necessary and sufficient condition of dynamical stability, since the ‘compatibility criterion’ is not ‘appropriately’ satisfied by the equilibrium configurations.

Step (4): We would re-construct the NS sequences described in steps (2) and (3) respectively for an ‘appropriate’ boundary value of $(P_b/E_b) = (P_b/E_b)_2$ (say). Since for this particular value of (P_b/E_b) , The ‘compatibility criterion’ turns out to be ‘appropriately’ satisfied by all the equilibrium sequences corresponding to an envelope with $\Gamma_1 = 4/3, 5/3$ and 2 respectively, it would follow that the $M - R$ relation does provide the necessary and sufficient condition of dynamical stability for the said sequences [the value $(P_b/E_b)_2$ corresponds to the *minimum* value of (P_b/E_b) for which the $M - R$ relation fulfills the necessary and sufficient condition of dynamical stability for the equilibrium sequence corresponding to NS models with an envelope $\Gamma_1 = 2$. Since the value $(P_b/E_b)_2$ turns out to be greater than $(P_b/E_b)_1$, it follows, therefore, that this particular value $(P_b/E_b)_2$ would guarantee the automatic fulfillment of the ‘compatibility criterion’ for all the sequences corresponding to NS models with an envelope $\Gamma_1 = 4/3, 5/3$ and 2 respectively, together with fulfilling the necessary and sufficient condition of dynamical stability provided by the $M - R$ relation. This condition is termed as the ‘appropriate’ fulfillment of ‘compatibility criterion’].

The methodology regarding the construction of various models mentioned in steps (1) - (4) above and the important outcome emerging thereafter are discussed in the following section.

The assignment of different values of Γ_1 between the range (4/3) and 2 in the envelope of NS models discussed under step (2) to step (4) above follows from the fact that (4/3) represents the EOS of ultrarelativistic degenerate electrons and non-relativistic nuclei (Chandrasekhar 1935) or of relativistic degenerate neutron gas (Zeldovich & Novikov 1978). (5/3) corresponds to the well known EOS of non-relativistic degenerate neutrons gas (Oppenheimer & Volkoff 1939) and $\Gamma_1 = 2$ represents the case of extreme relativistic baryons interacting through vector meson field (Zeldovich 1962) [The value of $\Gamma_1 > 2$ is also possible for some EOS, e.g., Mal-

one, Johnson & Bethe (1975); Clark, Heintzmann & Grewing (1971), however, the results obtained in this paper do not get affected by choosing $\Gamma_1 > 2$]. The various values of Γ_1 chosen in this range ($4/3 \leq \Gamma_1 \leq 2$) can cover almost all of the nuclear EOS discussed in the literature (and, therefore, it can cover almost full range of nuclear density which might be applicable for the envelope region as well), and in our opinion, it could be more appropriate to choose an average (constant) value of Γ_1 for a conventional NS model, instead of going into the details of the density range below E_b specified by different EOS [for example, BPS, NV, or FPS (Lorenz, Ravenhall & Pethick 1993)] which are frequently used by various authors in the conventional models of neutron stars in spite of their uncertainty (Friedman & Ipser 1987; Dolan 1992) as mentioned earlier. The EOS of classical polytrope for the said Γ_1 values, considered in the present study, will not only simplify the procedure but also provide necessary insight regarding the suitability of the EOS for the envelope region, since this study yields the important finding that the stable sequences of neutron star models terminate at the same value of maximum mass independent of the EOS of the envelope.

3 METHODOLOGY AND DISCUSSION

The metric for spherically symmetric and static configurations can be written in the following form (remembering that we are using geometrized units, i.e. $G = c = 1$; where G and c represent respectively, the universal constant of gravitation and the speed of light in vacuum)

$$ds^2 = e^\nu dt^2 - e^\lambda dr^2 - r^2 d\theta^2 - r^2 \sin^2 \theta d\phi^2, \quad (2)$$

where ν and λ are functions of r alone. The Oppenheimer-Volkoff (O-V) equations (Oppenheimer & Volkoff 1939), resulting from Einstein’s field equations, for systems with isotropic pressure P and energy-density E can be written as

$$P' = -(P + E)[4\pi Pr^3 + m]/r(r - 2m) \quad (3)$$

$$\nu'/2 = -P'/(P + E) \quad (4)$$

$$m'(r) = 4\pi Er^2; \quad (5)$$

where $m(r) = \int_0^r 4\pi Er^2 dr$ is the mass, contained within the radius r , and the prime denotes radial derivative.

In order to solve equations (3) - (5) for different models considered in the present study, we consider the stiffest EOS

$$P = E - E_s, \quad (6)$$

for the entire configuration (or for the core region), and the EOS of classical polytrope

$$\frac{d \ln P}{d \ln \rho} = \Gamma_1 \quad (7)$$

for the envelope region respectively. For core-envelope models, the fractional moment of inertia (given by equation (1)) may be calculated by using an approximate but very precise empirical formula which is based on 30 theoretical EOSs of dense nuclear matter. For NS models, the formula yields in the following form (Bejger & Haensel 2002)

$$I \simeq \frac{2}{9}(1 + 5x)MR^2, \quad x > 0.1 \quad (8)$$

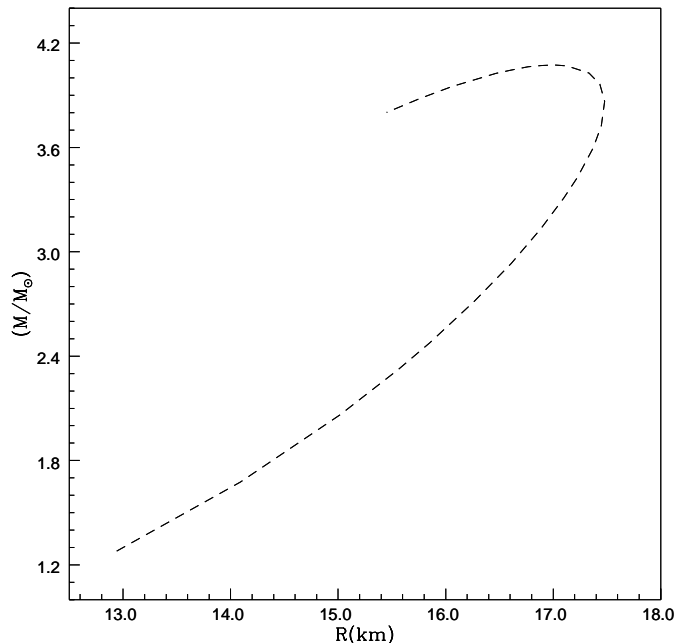


Figure 1. The mass-radius diagram of the models corresponding to the stiffest EOS, $P = (E - E_s)$, (as discussed in the text (step 1, sections 2 and 3)) for an assigned value of the density $E_s = 2.7 \times 10^{14} \text{ g cm}^{-3}$ at the surface. The models do not fulfill the ‘compatibility criterion’ as shown in Table 1. Also, the mass-radius diagram does not provide the necessary and sufficient condition of dynamical stability because the inequalities, $(\Gamma_1)_0 \leq 2.5946$ and $u_{\text{max}} \leq 0.3406$, are not fulfilled simultaneously at the maximum value of mass as shown in Table 1.

where x is the compactness parameter measured in units of $[M_\odot (\text{km})/\text{km}]$, i.e.

$$x = \frac{M/R}{M_\odot/\text{km}} = \frac{u}{1.477}. \quad (9)$$

In accordance with the four step consecutive study mentioned in the last section, we construct different models in the following manner

Models mentioned in step (1): The coupled equations (3 - 5) are solved for the EOS given by equation (6) until pressure vanishes at the surface of the configuration for a fiduciary choice of $E_s = 2.7 \times 10^{14} \text{ g cm}^{-3}$, the nuclear saturation density. At the surface, $r = R$, we obtain $P = 0$, $E = E_s$, $m(r = R) = M$, $e^\nu = e^{-\lambda} = (1 - 2M/R) = (1 - 2u)$. The results of the calculations are shown in Table 1 and the $M - R$ diagram is presented in Fig.1. It follows from Table 1 that along the stable branch of the sequence, the maximum value of mass corresponds to the maximum ‘stable’ value of $u_{\text{max}} \simeq 0.3539$ and the corresponding ‘local’ value of $(\Gamma_1)_0 \simeq 2.4990$. Although, this value of $(\Gamma_1)_0$ turns out to be consistent with that of the absolute upper bound on $(\Gamma_1)_0$ ($(\Gamma_1)_{0,\text{max,abs}} \simeq 2.5946$), the maximum ‘stable’ value of $u_{\text{max}} \simeq 0.3539$ is found to be inconsistent with that of the absolute upper bound on u_{max} ($u_{\text{max,abs}} \simeq 0.3406$). Thus the configuration turns out to be inconsistent with the corollary 1 of Theorem 2 (Negi 2007). It follows, therefore, that the $M - R$ relation corresponding to the stiffest EOS does not

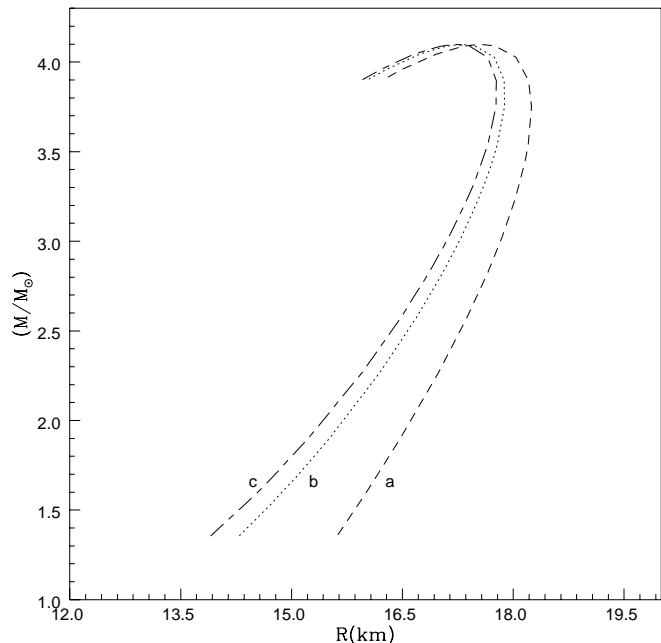


Figure 2. The mass-radius diagram of the models as discussed in the text (steps (2) and (3), sections 2 and 3) for an assigned value of matching density $E = E_b = 2.7 \times 10^{14} \text{ g cm}^{-3}$ at the core-envelope boundary. The labels a, b and c represent the models for an envelope with $\Gamma_1 = (4/3), (5/3)$, and 2 respectively. The value of the ratio of pressure to energy-density, $(P_b/E_b) = (P_b/E_b)_1 = 1.0645 \times 10^{-2}$, at the core envelope boundary is assigned in such a manner that the ‘compatibility criterion’ has become satisfied by all the models corresponding to an envelope with $\Gamma_1 = 4/3$, whereas it remains unsatisfied by various models corresponding to an envelope with $\Gamma_1 = 5/3$ and 2 respectively as shown in Table 3. Since, the ‘compatibility criterion’ has not been satisfied ‘appropriately’ by the models corresponding to an envelope with $\Gamma_1 = 4/3$ (and has not been satisfied by various models corresponding to an envelope with $\Gamma_1 = 5/3$ and 2), the $M - R$ relation does not provide the necessary and sufficient condition of dynamical stability for any sequence as shown in Table 2.

provide the necessary and sufficient condition of dynamical stability for the equilibrium configurations. Since, the total mass ‘ M ’ which appears here does not fulfill the definition of the ‘actual mass’ which should be present in the exterior Schwarzschild solution (Negi 2004; 2006), the equilibrium sequence corresponding to the pure stiffest EOS, therefore, does not even fulfill the necessary condition of hydrostatic equilibrium (Negi 2007), as a result the ‘compatibility criterion’ can not be made satisfied by such configurations. This is also evident from the comparison of column 2 and 6 of Table 1 that for each assigned value of (P_0/E_0) , $u_{\text{stff}} > u_h$.

Models mentioned in step (2): The coupled equations (3 - 5) are solved by considering equation (6) in the core ($0 \leq r \leq b$) and equation (7) in the envelope ($b \leq r \leq R$) for the constant $\Gamma_1 = 5/3$ and 2 respectively, until the boundary conditions: $P = E = 0$, $m(r = R) = M$, $e^\nu = e^{-\lambda} = (1 - 2M/R) = (1 - 2u)$ are reached at the surface, $r = R$, of the configuration. Equation (8) is also used together with equations (3 - 5) to calculate the fractional mo-

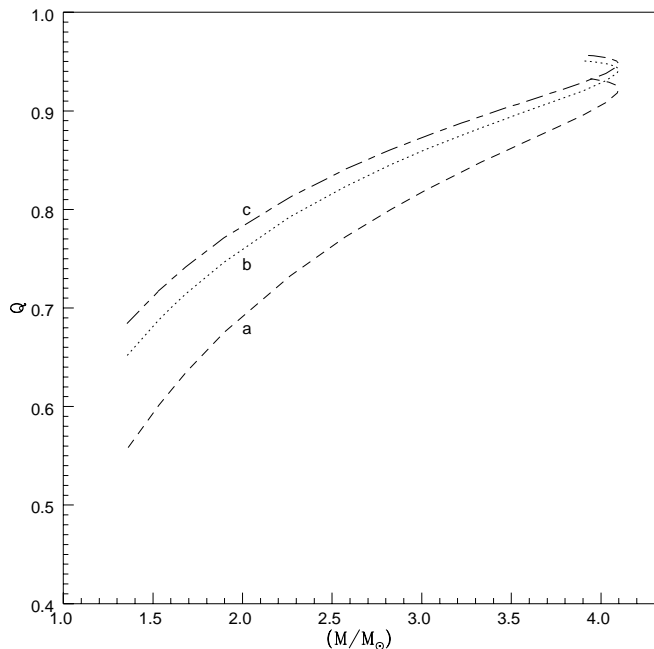


Figure 3. Fractional moment of inertia $Q(\equiv I_{\text{core}}/I_{\text{total}})$ vs. total mass M for the models presented in Tables 2 and 3 and shown in Figure 2. The labels a, b and c denote the models for an envelope with $\Gamma_1 = (4/3), (5/3),$ and 2 respectively.

ment of inertia given by equation (1) and the moment of inertia of the entire core-envelope model considered in the present section. The calculations are performed for a fiduciary choice of the boundary density, $E_b = 2.7 \times 10^{14} \text{ g cm}^{-3}$, and for an ‘arbitrarily’ assigned value of the ratio of pressure to energy-density at the core-envelope boundary, $(P_b/E_b) = (P_b/E_b)_1 = 1.0645 \times 10^{-2}$. The results of the calculations are summarized in Tables 2 - 3 (indicated with a superscript ‘b’ for the $\Gamma_1 = 5/3$ and ‘c’ for the $\Gamma_1 = 2$ envelope models) and the $M - R$ diagram is shown in Fig.2 (label ‘b’ for the $\Gamma_1 = 5/3$ and ‘c’ for the $\Gamma_1 = 2$ envelope models). Though, the construction of such core-envelope models appropriately fulfill the definition of the ‘actual mass’ appearing in the exterior Schwarzschild solution (Negi 2007), the choice of $(P_b/E_b) = (P_b/E_b)_1$, however, yields the sequences (corresponding to NS models with an envelope $\Gamma_1 = 5/3$ and 2 respectively) which fulfill only the necessary (but not sufficient) condition of hydrostatic equilibrium, since the ‘compatibility criterion’ remains unsatisfied by such sequences as shown in Table 3. From the Table 2, we find that at the maximum mass values along the stable branch of the sequences, the sequence composed of NS models with an envelope $\Gamma_1 = 5/3$ yields $u_{\text{max}} \simeq 0.3493$ and the corresponding value of $(\Gamma_1)_0 \simeq 2.4984$, whereas the sequence composed of NS models with an envelope $\Gamma_1 = 2$ yields $u_{\text{max}} \simeq 0.3509$ and the corresponding value of $(\Gamma_1)_0 \simeq 2.4984$ respectively. Both pairs of these values are, however, found to be inconsistent with that of the pair of absolute upper bounds $u_{\text{max,abs}}(\simeq 0.3406)$ and $(\Gamma_1)_{0,\text{max,abs}}(\simeq 2.5946)$ respectively. It follows, therefore, that the $M - R$ relation corresponding to the sequences (composed of NS models with an envelope

$\Gamma_1 = 5/3$ and 2 respectively) does not provide the necessary and sufficient condition of dynamical stability as shown in Fig.2.

Tables 2 - 3 and Fig.3 show that the range of fractional moment of inertia, $0.652 \leq Q \leq 0.948$, corresponding to the ‘stable’ models (with an envelope $\Gamma_1 = 5/3$ and 2 respectively) possesses the NS masses in the range $1.35M_\odot \leq M \leq 4.1M_\odot$. This feature is consistent with those of the conventional models discussed in the literature and can explain only the higher values of the glitch healing parameter observed for the Crab-like pulsars. However, for the minimum weighted mean value of $Q \simeq 0.7$ corresponding to the Crab pulsar, we obtain from Fig.3, the minimum masses $M_b \simeq 1.6M_\odot$ and $M_c \simeq 1.44M_\odot$ for the Crab pulsar.

Models mentioned in step (3): In order to construct core-envelope models corresponding to the constant $\Gamma_1 = 4/3$ for the envelope, we use equation (7) for the envelope ($b \leq r \leq R$) and equation (6) for the core ($0 \leq r \leq b$) and solve equations (3 - 5) together with equation (8) for the same boundary conditions mentioned in the last sub-section (step (2)) for the surface and the core-envelope boundary, viz. $E_b = 2.7 \times 10^{14} \text{ g cm}^{-3}$, and $(P_b/E_b) = (P_b/E_b)_1 = 1.0645 \times 10^{-2}$ respectively. The various parameters obtained for this model are indicated with a superscript ‘a’ in Tables 2 and 3 respectively, and the $M - R$ diagram (marked with label ‘a’) is presented in Fig.2. Table 3 shows that although the ‘compatibility criterion’ is satisfied by all members of the sequence corresponding to NS models with an envelope $\Gamma_1 = 4/3$ for the choice of the boundary condition $(P_b/E_b) = (P_b/E_b)_1$, this choice, however, does not appear to be ‘appropriate’ because at the maximum value of mass along the stable branch of the sequence in the mass-radius relation, the model yields the maximum value of $u(u_{\text{max}}) \simeq 0.3444$ and the corresponding value of $(\Gamma_1)_0 \simeq 2.4984$ as shown in Table 2. These values, however, show inconsistency with that of the pair of absolute upper bounds, $u_{\text{max,abs}}(\simeq 0.3406)$ and $(\Gamma_1)_{0,\text{max,abs}}(\simeq 2.5946)$, respectively. It follows from this result that the necessary and sufficient condition of dynamical stability (provided by the $M - R$ relation) may remain unsatisfied even when all members of the sequence do satisfy the ‘compatibility criterion’.

Tables 2 - 3 and Fig.3 also indicate that the range of fractional moment of inertia, $0.558 \leq Q \leq 0.922$, for the ‘stable’ sequence corresponding to the $\Gamma_1 = 4/3$ envelope model provides the masses of NS models in the range, $1.36M_\odot \leq M \leq 4.1M_\odot$. These higher values of the glitch healing parameter are consistent only with those the Crab-like pulsars as discussed in the last sub-section (step 2). However, for the minimum value of $Q \simeq 0.7$, Fig.3 yields the minimum mass $M_c \simeq 2.03M_\odot$ for the Crab pulsar.

Models mentioned in step (4): We re-construct the NS sequences (composed of core-envelope models), those described in the last two sub-sections (steps (2) and (3) respectively), but for an ‘appropriate’ value of $(P_b/E_b) = (P_b/E_b)_2 = 4.694 \times 10^{-2}$. The results of the calculations are summarized in Tables 4 - 5 and the $M - R$ diagram is shown in Fig.4. The superscripts ‘a’, ‘b’ and ‘c’ which appear among various parameters in these tables, represent the models with an envelope $\Gamma_1 = 4/3, 5/3$ and 2 respectively. The $M - R$ diagram is also labeled in the similar fashion. The value $(P_b/E_b)_2$, in fact, represents the *minimum* value of (P_b/E_b) for which *all* the sequences, corresponding to NS

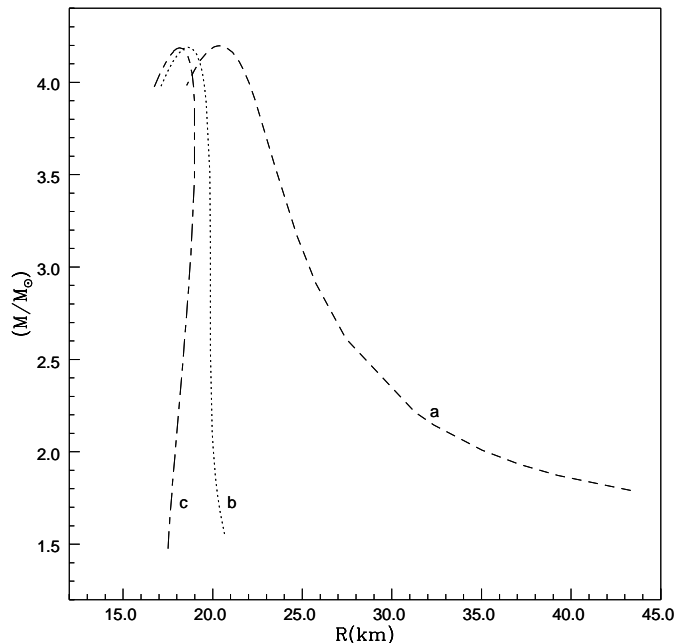


Figure 4. The mass-radius diagram of the models as discussed in the text (step 4, sections 2 and 3) for an assigned value of matching density $E = E_b = 2.7 \times 10^{14} \text{ g cm}^{-3}$ at the core-envelope boundary. The labels a, b and c represent the models for an envelope with $\Gamma_1 = (4/3), (5/3)$, and 2 respectively. The value of the ratio of pressure to energy-density, $(P_b/E_b) = (P_b/E_b)_2 = 4.694 \times 10^{-2}$, at the core envelope boundary is obtained in such a manner that the ‘compatibility criterion’ is ‘appropriately’ satisfied by *all* the models corresponding to an envelope with $\Gamma_1 = 4/3, 5/3$ and 2 respectively, as shown in Table 5. That is, the necessary and sufficient condition of dynamical stability provided by the $M - R$ relation is also satisfied together with satisfying the ‘compatibility criterion’ as shown in Table 4.

models with an envelope $\Gamma_1 = 4/3, 5/3$ and 2 respectively, fulfill the necessary and sufficient condition of dynamical stability provided by the $M - R$ relation. Since the value $(P_b/E_b)_2 > (P_b/E_b)_1$, it follows that the ‘compatibility criterion’ would automatically be satisfied by *all* the sequences corresponding to NS models with an envelope $\Gamma_1 = 4/3, 5/3$ and 2 respectively. This is evident from the Tables 4 and 5 respectively. A comparison of column 2 with those of column 3, 4 and 5 of Table 5 show that the ‘compatibility criterion’ is ‘appropriately’ satisfied by all the sequences. Table 4 shows that at the maximum values of mass along the stable branch of the sequences, the models corresponding to an envelope with $\Gamma_1 = 4/3, 5/3$ and 2 yield the maximum values of $u(u_{\text{mas}}) \simeq 0.3044, 0.3324$ and 0.3404 respectively for the same value of $(\Gamma_1)_0 \simeq 2.4955$. Evidently, these values are consistent with those of the absolute upper bounds $u_{\text{max,abs}} (\simeq 0.3406)$ and $(\Gamma_1)_{0,\text{max,abs}} (\simeq 2.5946)$ respectively.

Tables 4 - 5 and Fig.5 show that the ranges of fractional moment of inertia, $0.069 \leq Q \leq 0.779$, obtained for the stable sequences corresponding to the $\Gamma_1 = 5/3$ and 2 envelope models have masses in the range, $1.48M_\odot \leq M \leq 4.2M_\odot$. Obviously, these ranges are capable of fulfilling the higher as well as lower values of the glitch healing parameter cor-

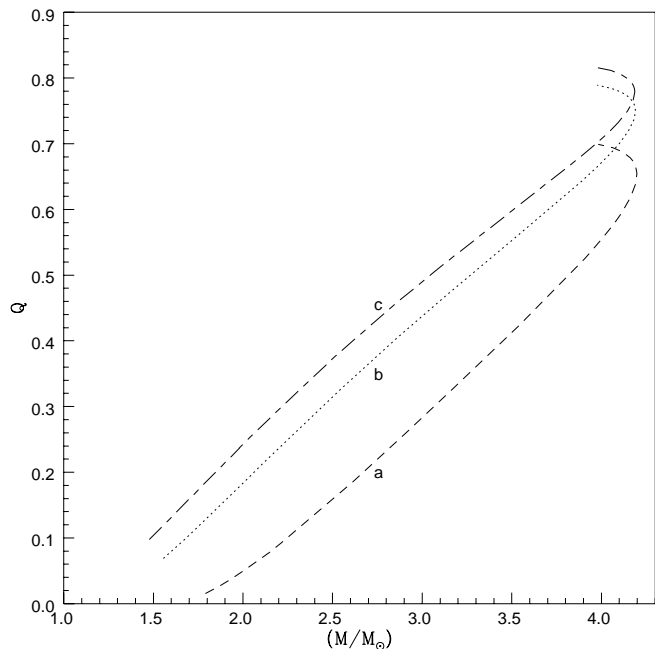


Figure 5. Fractional moment of inertia $Q (\equiv I_{\text{core}}/I_{\text{total}})$ vs. total mass M for the models presented in Tables 4 and 5 and shown in Figure 4. The labels a, b and c denote the models for an envelope with $\Gamma_1 = (4/3), (5/3)$, and 2 respectively.

responding to the case of the Crab and the Vela-like pulsars respectively. For the maximum weighted mean value of $Q \simeq 0.2$ corresponding to the Vela pulsar, Fig.5 yields the maximum masses $M_b \simeq 2.06M_\odot$ and $M_c \simeq 1.85M_\odot$ for the Vela pulsar, whereas for the minimum weighted mean value of $Q \simeq 0.7$, the models yield the minimum masses $M_b \simeq 4.1M_\odot$ and $M_c \simeq 3.98M_\odot$ for the Crab pulsar respectively. It also follows from the Tables 4 - 5 and Fig.5 that for the stable range of fractional moment of inertia, $0.016 \leq Q \leq 0.655$, corresponding to the $\Gamma_1 = 4/3$ envelope models, the NSs can have masses in the range, $1.79M_\odot \leq M \leq 4.2M_\odot$. For the maximum weighted mean value of $Q \simeq 0.2$, Fig.5 yields the maximum mass $M_c \simeq 2.67M_\odot$ for the Vela pulsar, however the minimum weighted mean value, $Q \simeq 0.7$, corresponds to the minimum mass, $M_a \simeq 3.98M_\odot$, for the Crab pulsar which lies in the unstable branch of Fig.5.

The important conclusions emerge from the four step study and discussion presented above may be summarized in the following manner:

(1) Steps (1), (2) and (4) show that the $M - R$ relation provides the necessary and sufficient condition of dynamical stability only when the ‘compatibility criterion’ for the equilibrium configurations is satisfied. Without satisfying the ‘compatibility criterion’, the $M - R$ relation can not provide the necessary and sufficient condition of dynamical stability.

(2) The inclusion of step (3), however, modifies the above conclusion in the following statement: The $M - R$ relation provides the necessary and sufficient condition of dynamical stability only when the ‘compatibility criterion’ is ‘appropriately’ satisfied. Thus, the necessary and suffi-

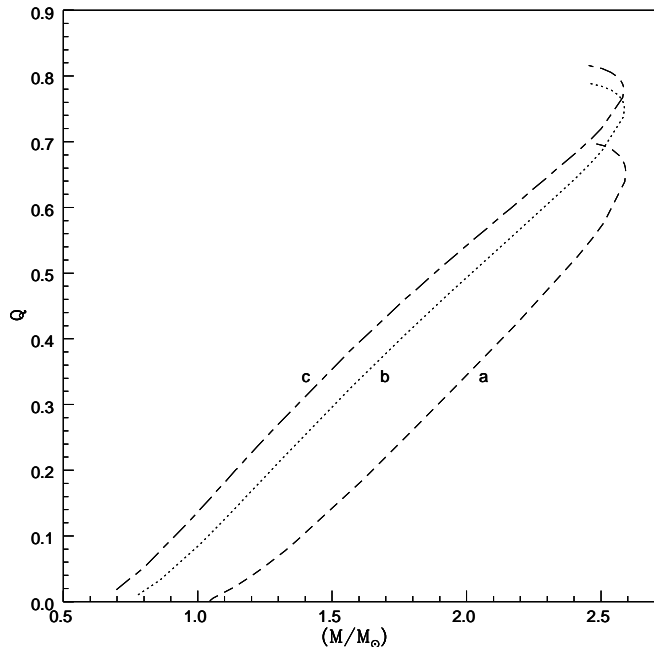


Figure 6. Fractional moment of inertia $Q(\equiv I_{\text{core}}/I_{\text{total}})$ vs. total mass M for the models as discussed in the text (step 4, section 2 and 3) for a *calculated* value of matching density $E = E_b = 7.0794 \times 10^{14} \text{ g cm}^{-3}$ at the core-envelope boundary. The labels a, b and c represent the models for an envelope with $\Gamma_1 = (4/3), (5/3)$, and 2 respectively. The value of the ratio of pressure to energy-density, $(P_b/E_b) = (P_b/E_b)_2 = 4.694 \times 10^{-2}$, at the core envelope boundary is obtained in such a manner that the ‘compatibility criterion’ is ‘appropriately’ satisfied for *all* the models corresponding to an envelope with $\Gamma_1 = 4/3, 5/3$ and 2 respectively (in the same manner as shown in Table 5 for the matching density $E = E_b = 2.7 \times 10^{14} \text{ g cm}^{-3}$ at the core-envelope boundary). That is, the necessary and sufficient condition of dynamical stability provided by the $M - R$ relation is also satisfied together with satisfying the ‘compatibility criterion’ (in the same manner as shown in Table 4 for the matching density $E = E_b = 2.7 \times 10^{14} \text{ g cm}^{-3}$ at the core-envelope boundary).

cient condition provided by the $M - R$ relation is totally dependent on the ‘appropriate’ fulfillment of ‘compatibility criterion’. On the other hand, the fulfillment of ‘compatibility criterion’ is quite independent of the fulfillment of necessary and sufficient condition of dynamical stability provided by the $M - R$ relation, because the ‘compatibility criterion’ can be made satisfied even without fulfilling the necessary and sufficient condition of dynamical stability provided by the $M - R$ relation. Since, the fulfillment of the ‘compatibility criterion’ alone is a measure of the fulfillment of necessary and sufficient condition of hydrostatic equilibrium for any static and spherical configuration (Negi 2007), it follows from the above discussion that the fulfillment of the ‘compatibility criterion’ alone, independently provides, in general, the necessary and sufficient condition of hydrostatic equilibrium for any sequence composed of regular, static and spherical configurations.

4 RESULTS AND CONCLUSIONS

We have investigated that the mass-radius relation corresponding to the stiffest equation of state does not provide the necessary and sufficient condition of dynamical stability because at the maximum value of mass along the mass-radius relation, the pair of the maximum ‘stable’ value of compactness, $u_{\text{max}} \simeq 0.3539$, and the corresponding central value of the ‘local’ adiabatic index, $(\Gamma_1)_0 \simeq 2.4990$, turns out to be inconsistent with that of the pair of *absolute* values, $u_{\text{max,abs}} \simeq 0.3406$, and $(\Gamma_1)_{0,\text{max,abs}} \simeq 2.5946$, compatible with the structure of general relativity, causality, and dynamical stability. The reason behind this inconsistency lies in the fact that the ‘compatibility criterion’ (Negi and Durgapal 2001) can not be fulfilled by any of the sequence, composed of regular configurations corresponding to a *single* EOS with finite (non-zero) values of surface and central density (Negi 2004; 2006).

We have further constructed the sequences composed of core-envelope models such that, like the stiffest EOS, each member of these sequences satisfy the extreme case of causality condition, $v = c = 1$, at the centre by considering the stiffest equation of state in the core and a polytropic equation with the constant adiabatic index $\Gamma_1 = [d \ln P / d \ln \rho]$ in the envelope and investigated the resulting configurations on the basis of the ‘compatibility criterion’ and the mass-radius relation for different values of $\Gamma_1 = 4/3, 5/3$ and 2. Together with the finding corresponding to the case of stiffest EOS mentioned above, the investigation of the said sequences of the core-envelope models explicitly show that the mass-radius relation corresponding to the said sequences can provide the necessary and sufficient condition of dynamical stability only when the ‘compatibility criterion’ for the sequences in ‘appropriately’ satisfied. However, the fulfillment of ‘compatibility criterion’ can remain satisfied even when the mass-radius relation does not provide the necessary and sufficient condition of dynamical stability for the equilibrium configurations.

In continuation to the results of previous study (Negi 2007), these results explicitly show that the ‘compatibility criterion’ *independently* provides, in general, the *necessary* and *sufficient* condition of hydrostatic equilibrium for any regular sequence.

The causal sequences of NS models constructed in the present study (which fulfill the necessary and sufficient condition of hydrostatic equilibrium and dynamical stability simultaneously) terminate at the same value of maximum mass, $M_{\text{max}} \approx 4.2 M_{\odot}$ (for $E_b = 2.7 \times 10^{14} \text{ g cm}^{-3}$), independent of the EOS of the envelope. However, the maximum compactness, $u_{\text{max}} \simeq 0.3404$, yields for the sequence corresponding to the $\Gamma_1 = 2$ envelope models. While for the the same value of transition density $E_b = 2.7 \times 10^{14} \text{ g cm}^{-3}$ at the core-envelope boundary, this upper bound on NS mass found to be fully consistent with those of the models formulated with the advance nuclear theory (Kalogera & Baym 1996), the $\Gamma_1 = 2$ envelope model indicates the appropriateness of the (average) value of Γ_1 for the entire envelope.

Beside its fundamental feature, this study also underlines the importance of the applicability of ‘compatibility criterion’ to the conventional models of NSs. Since, we find that when the ‘compatibility criterion’ is not satisfied (for the case of the models corresponding to an envelope with

$\Gamma_1 = 5/3$ and 2, if the ratio of pressure to energy-density at the core-envelope boundary, P_b/E_b , is ‘arbitrarily’ assigned to be about 1.0645×10^{-2}) or not ‘appropriately’ satisfied (for the case of the models corresponding to an envelope with $\Gamma_1 = 4/3$, if $P_b/E_b \simeq 1.0645 \times 10^{-2}$) by the sequences, the corresponding range of the glitch healing parameter turns out to be $0.558 \leq Q \leq 0.948$. This feature is consistent with the other conventional NS models discussed in the literature and can explain only the higher values of Q on the basis of starquake model of glitch generation for the Crab-like pulsars. For the minimum weighted mean value of $Q \simeq 0.7$, our models (corresponding to an envelope with $\Gamma_1 = 2, 5/3$ and $4/3$ respectively) yield the minimum masses $M_c \simeq 1.44M_\odot$, $M_b \simeq 1.6M_\odot$ and $M_a \simeq 2.03M_\odot$ for the Crab pulsar. Among these values, the first two values are comparable with those of the minimum values $1.35M_\odot$ and $1.65M_\odot$ obtained by Crawford and Demiański (2003) by using the GWM (Glendenning, Weber, & Moszkowski 1992) and HKP (Haensel, Kutschera, & Proszynski 1981) EOSs. Whereas, corresponding to $Q \simeq 0.7$, the other five EOSs of the dense nuclear matter considered by Crawford and Demiański (2003) yield the minimum mass $M < 1M_\odot$ for the Crab pulsar (see, e.g. Crawford and Demiański 2003; and references therein). However for the maximum weighted mean value of $Q \simeq 0.2$ corresponding to the Vela pulsar, our models also yield the unrealistically small mass values for the Vela pulsar together with the other models discussed in the literature (Crawford and Demiański 2003).

On the other hand, as soon as the ‘compatibility criterion’ is ‘appropriately’ satisfied by all the models corresponding to an envelope with $\Gamma_1 = 4/3, 5/3$ and 2 respectively (that is, if the ratio of pressure to energy-density at the core-envelope boundary, P_b/E_b , is set (and not ‘arbitrarily’ assigned) to be about 4.694×10^{-2} for all the sequences), the corresponding range of the glitch healing parameter turns out to be $0.016 \leq Q \leq 0.779$. This range, however, can explain both (the higher as well as lower) values of Q on the basis of starquake model of glitch generation for the Crab, as well as for the Vela-like pulsars. The sequences corresponding to an envelope with $\Gamma_1 = 5/3$ and 2 yield the maximum masses $M_b \simeq 2.06M_\odot$, $M_c \simeq 1.85M_\odot$ for the Vela ($Q \simeq 0.2$) and the minimum masses $M_b \simeq 4.1M_\odot$, $M_c \simeq 3.98M_\odot$ for the Crab ($Q \simeq 0.7$) pulsar respectively. The sequence corresponding to an envelope with $\Gamma_1 = 4/3$, however, yields the maximum mass $M_a \simeq 2.67M_\odot$ for the Vela pulsar ($Q \simeq 0.2$) but it does not provide the minimum stable mass for the Crab pulsar as soon as the constraint of $Q \geq 0.7$ is imposed.

The higher mass values mentioned in the last paragraph for the Crab pulsar seem to be unlikely, since none of the observational and/or the theoretical study predict such higher mass values for the Crab pulsar. Thus, unlike the results of steps 2 - 3 (section 3) which deal with the study of NS models without implementing the ‘appropriate’ fulfillment of ‘compatibility criterion’, the implementation of the ‘appropriate’ fulfillment of ‘compatibility criterion’ also reveals that in order to construct a ‘realistic’ NS sequence composed of NS masses comparable with those of the observations, we have to modify the value of matching density at the core-envelope boundary. In view of the modern EOSs of dense nuclear matter, the upper bound on NS mass compatible with causality and dynamical stability can reach up to a value as large as $2.2M_\odot$, since among the variety of mod-

ern EOSs discussed in the literature only the following EOSs yield the maximum mass of NS model in excess of $2M_\odot$: SLy (Douchin & Haensel 2001) EOS, $M_{\max} = 2.05M_\odot$; BGN1 (Balberg & Gal 1997) EOS, $M_{\max} = 2.18M_\odot$; and APR (Akmal et. al. 1998) EOS, $M_{\max} = 2.21M_\odot$ (see, e.g. Haensel et al 2006). However, on the basis of other modern EOSs for NS matter, fitted to experimental nucleon-nucleon scattering data and the properties of light nuclei, Kalogera & Baym (1996; and references therein) have also shown that the lowest possible upper bound on NS mass, compatible with causality and dynamical stability, corresponds to the value of $2.2M_\odot$ which can exceed up to a value as large as $2.9M_\odot$. Considering their mean $\sim 2.6M_\odot$ as the most likely recent value to the upper bound on NS masses and substituting this value as an upper bound to our models mentioned in step 4 of section 3, we obtain the ‘appropriate’ value of matching density $E_b = 7.0794 \times 10^{14} \text{ g cm}^{-3}$ at the core-envelope boundary. On the basis of this density, our reconstructed sequences (corresponding to an envelope with $\Gamma_1 = 5/3$ and 2 respectively) yield the maximum masses $M_b \simeq 1.28M_\odot$, $M_c \simeq 1.14M_\odot$ for the Vela ($Q \simeq 0.2$) and the minimum masses $M_b \simeq 2.53M_\odot$, $M_c \simeq 2.45M_\odot$ for the Crab ($Q \simeq 0.7$) pulsar as shown in Fig.6. The sequence corresponding to an envelope with $\Gamma_1 = 4/3$, however, yields the maximum mass $M_a \simeq 1.66M_\odot$ for the Vela pulsar ($Q \simeq 0.2$) but as shown in Fig.6, the minimum mass of the Crab pulsar ($M_a \approx 2.46M_\odot$) belongs to the unstable branch of the sequence as soon as the constraint of $Q \geq 0.7$ is imposed. Obviously, the other conclusions of the present study, drawn on the basis of assigning the fiduciary density $E_b = 2.7 \times 10^{14} \text{ g cm}^{-3}$ at the boundary will remain unaltered.

ACKNOWLEDGMENTS

The author gratefully acknowledges Prof. M. C. Durgapal for his valuable advice and discussion and the referee for his helpful comments and suggestion that improved the manuscript. The Aryabhata Research Institute of Observational Sciences (ARIES), Nainital is gratefully acknowledged for providing library and computer-centre facilities.

REFERENCES

- Akmal, A., Pandharipande, V. R., & Ravenhall, D. G., 1998, Phys. Rev. C 58, 1804 (APR)
- Arnett W. D., Bowers R. L., 1977, ApJ Suppl. 33, 415
- Balberg, S., & Gal A., 1997, Nucl. Phys. A 625, 435 (BGN1)
- Baym, G., Pethick, C., & Sutherland, P. 1971, ApJ, 170, 299 (BPS)
- Bejger, M., & Haensel, P. 2002, A&A 396, 917
- Brecher, K., & Caporaso, G., 1976, Nature 259, 377
- Chandrasekhar, S. 1935, MNRAS, 95, 207
- Clark, J. W. Heintzmann, H., & Grewing, M. 1971, Astrophys. Letters 10, 21
- Crawford, F., & Demiański, M. 2003, ApJ 595, 1052
- Dolan, J. F. 1992, ApJ 384, 249
- Douchin, F., & Haensel, P. 2001, A&A 380, 151 (SLy)
- Friedman, J. L., & Ipser, J. R. 1987, ApJ 314, 594
- Glendenning, N. K., Weber, F., & Moszkowski, S. A. 1992, Phys. Rev.C 45, 844 (GWM)
- Haensel, P., Kutschera, M., & Proszynski, M. 1981, A&A, 102, 299 (HKP)

- Haensel, P., Potekhin, A. Y., & Yakovlev, D. G. 2006, Neutron Stars 1 - Equation of State and Structure, Springer
- Haensel, P., & Zdunik J. L. 1989, Nature 340, 617
- Hartle, J. B. 1978, Phys. Rep. 46, 201
- Kalogera, V. & Baym, G. 1996, ApJ 470, L61
- Lee, T. D. 1975, Rev. Mod. Phys. 47, 267
- Lorenz, C. P., Ravenhall, D. G., & Pethick, C. J. 1993, Phys. Rev. Lett. 70, 379 (FPS)
- Malone, R. C., Johnson, M. B., & Bethe, H. A. 1975, ApJ 199, 741
- Negi, P. S. 2004, Mod. Phys. Lett. A 19, 2941 (astro-ph/0210018)
- Negi, P. S. 2006, Int. J. Theoretical Phys., 45, 1684 (gr-qc/0401024)
- Negi, P. S. 2007, Int. J. Mod. Phys. D. 16, 35 (astro-ph/0606022)
- Negi, P. S., & Durgapal, M. C. 2000, A&A 353, 641
- Negi, P. S., & Durgapal, M. C. 2001, Grav. & Cosmol. 7, 37 (astro-ph/0312516)
- Negele, J., & Vautherin, D. 1973, Nucl. Phys., A207, 298 (NV)
- Oppenheimer, J. R., & Volkoff G. M. 1939, Phys. Rev. 55, 374
- Rhoades, C. E. Jr., & Ruffini, R. 1974, Phys. Rev. Lett. 32, 324
- Tooper, R. F. 1965, ApJ, 142, 1541
- Zeldovich, Ya. B. 1962, Soviet Phys., JETP, 15, 1158
- Zeldovich, Ya. B., & Novikov I. D. 1978, Relativistic Astrophysics, Vol.1, Chicago Univ. Press, Chicago (Midway Reprint)

Table 1. Mass (M), size (R), compactness ratio ($u_{\text{stff}} \equiv M/R$) and the central value of the ‘local’ adiabatic index $(\Gamma_1)_0$ of the configuration for various values of the ratio of central pressure to central energy-density (P_0/E_0) as obtained by assigning a fiduciary value of the density at the surface, $E_s = 2.7 \times 10^{14} \text{ g cm}^{-3}$, for the stiffest EOS, $P = (E - E_s)$. It is seen that for each assigned value of P_0/E_0 , the inequality, $u_{\text{stff}} \leq u_h$ (where u_h represents the corresponding value of the compactness ratio for the homogeneous density distribution shown in column 2) always remains unsatisfied. The slanted values correspond to the limiting case upto which the configuration remains pulsationally ‘stable’.

(P_0/E_0)	u_h	$(\Gamma_1)_0$	(M/M_\odot)	$R(\text{km})$	u_{stff}
0.10142	0.14343	10.8600	1.27922	12.94001	0.14601
0.13324	0.17226	8.50526	1.67675	14.09223	0.17574
0.16786	0.19835	6.95734	2.06245	15.01761	0.20284
0.19416	0.21528	6.15039	2.32350	15.56089	0.22054
0.21115	0.22511	5.73597	2.47752	15.85387	0.23081
0.24024	0.24025	5.16250	2.71665	16.27046	0.24661
0.27013	0.25389	4.70192	2.93370	16.60906	0.26089
0.30125	0.26640	4.31950	3.13171	16.88386	0.27396
0.33330	0.27777	4.00030	3.30968	17.10014	0.28587
0.35708	0.28536	3.80049	3.42668	17.22415	0.29384
0.39796	0.29698	3.51282	3.59800	17.37210	0.30591
0.43484	0.30617	3.29970	3.72636	17.44888	0.31543
0.48584	0.31722	3.05829	3.86625	17.47830	0.32672
0.53423	0.32626	2.87185	3.96327	17.43511	0.33574
0.58144	0.33396	2.71987	4.02801	17.33372	0.34322
0.64065	0.34236	2.56092	4.06856	17.12608	0.35088
0.66710	0.34573	<i>2.49903</i>	<i>4.07480</i>	<i>17.00784</i>	<i>0.35386</i>
0.69032	0.34852	2.44860	4.07117	16.88677	0.35608
0.71136	0.35092	2.40576	4.06364	16.76655	0.35797
0.73537	0.35351	2.35986	4.04578	16.61160	0.35973
0.75592	0.35563	2.32289	4.02622	16.46719	0.36112
0.80562	0.36037	2.24128	3.94943	16.05711	0.36328
0.83608	0.36305	2.19606	3.88049	15.75788	0.36372

Table 2. Mass (M), size (R), compactness ratio ($u \equiv M/R$), and the ‘local’ value of adiabatic index at the centre, $(\Gamma_1)_0$, for different values of the ratio of central pressure to central energy-density, (P_0/E_0) , for the core-envelope models discussed in the text (steps (2) and (3), section 3). Various parameters are obtained by assigning a fiduciary value of $E_b = 2.7 \times 10^{14}$ g cm $^{-3}$ for an assigned value of the ratio of pressure to energy-density, $(P_b/E_b) = (P_b/E_b)_1 \simeq 1.0645 \times 10^{-2}$, at the core-envelope boundary. The superscripts a, b, and c which appear among various parameters represent the models corresponding to an envelope with $\Gamma_1 = 4/3, 5/3$, and 2 respectively. The slanted values correspond to the limiting case upto which the configurations remain pulsationally ‘stable’. It is seen that the $M - R$ relation does not provide the necessary and sufficient condition of dynamical stability for any of the sequence, since none of the sequences satisfy both of the inequalities, viz. $u_{\max} \leq 0.3406$ and $(\Gamma_1)_0 \leq 2.5946$, simultaneously at the maximum value of mass. Although, all members of the sequence corresponding to an envelope with $\Gamma_1 = 4/3$ fulfill the ‘compatibility criterion’, $u \leq u_h$ (where u_h represents the compactness ratio of homogeneous density sphere for the corresponding value of P_0/E_0) without fulfilling the necessary and sufficient condition of dynamical stability provided by the $M - R$ relation, various members in the stable (as well as unstable) branch of the sequences corresponding to an envelope with $\Gamma_1 = 5/3$ and 2 do not fulfill the ‘compatibility criterion’ together with the last condition provided by the $M - R$ relation as shown in Table 3. Thus, the assigned value of $(P_b/E_b) = (P_b/E_b)_1 \simeq 1.0645 \times 10^{-2}$ corresponds to the *minimum* value for which the ‘compatibility criterion’, in fact, is not ‘appropriately’ satisfied by the sequence corresponding to an envelope with $\Gamma_1 = 4/3$ as discussed in step (3) of section 3.

(P_0/E_0)	$(\Gamma_1)_0$	(M^a/M_\odot)	R^a (km)	u^a	(M^b/M_\odot)	R^b (km)	u^b	(M^c/M_\odot)	R^c (km)	u^c
0.10603	10.4316	1.36098	15.62864	0.12862	1.35663	14.29216	0.14020	1.35439	13.90263	0.14389
0.11977	9.34904	1.53480	15.90839	0.14250	1.53103	14.71551	0.15367	1.52908	14.36231	0.15725
0.12544	8.97211	1.60425	16.02166	0.14789	1.60069	14.87248	0.15897	1.59885	14.54034	0.16241
0.13235	8.55591	1.68726	16.14566	0.15435	1.68392	15.06058	0.16514	1.68218	14.73637	0.16860
0.15071	7.63515	1.89840	16.46722	0.17027	1.89555	15.50498	0.18057	1.89405	15.21041	0.18390
0.18604	6.37510	2.26582	16.98853	0.19699	2.26364	16.18761	0.20654	2.26249	15.94411	0.20959
0.22012	5.54289	2.57456	17.37250	0.21889	2.57282	16.68887	0.22770	2.57189	16.47563	0.23056
0.25219	4.96523	2.82777	17.65613	0.23655	2.82633	17.04811	0.24486	2.82554	16.85773	0.24756
0.28047	4.56547	3.02420	17.84883	0.25025	3.02296	17.29460	0.25817	3.02230	17.12592	0.26065
0.31322	4.19268	3.22347	18.01620	0.26427	3.22240	17.51592	0.27172	3.22181	17.35701	0.27416
0.33333	4.00000	3.33234	18.08938	0.27209	3.33138	17.61968	0.27926	3.33085	17.47471	0.28153
0.35897	3.78575	3.45739	18.16419	0.28113	3.45653	17.72636	0.28801	3.45603	17.58420	0.29029
0.37791	3.64616	3.54070	18.20241	0.28730	3.53990	17.78229	0.29402	3.53946	17.65346	0.29613
0.43583	3.29448	3.75240	18.24864	0.30371	3.75176	17.88056	0.30991	3.75139	17.76321	0.31193
0.48898	3.04509	3.89663	18.20641	0.31612	3.89610	17.87641	0.32191	3.89580	17.76979	0.32381
0.56150	2.78094	4.02745	18.03557	0.32982	4.02703	17.74399	0.33521	4.02677	17.64993	0.33697
0.63427	2.57662	4.09052	17.74603	0.34045	4.09018	17.48404	0.34553	4.08998	17.40243	0.34713
0.66738	2.49839	4.09795	17.57442	0.34440	4.09764	17.32866	0.34926	4.09745	17.24674	0.35090
0.68401	2.46197	4.09650	17.48041	0.34613	4.09620	17.23688	0.35100	4.09604	17.16103	0.35253
0.70503	2.41839	4.08963	17.34875	0.34817	4.08935	17.11346	0.35294	4.08917	17.03632	0.35452
0.71465	2.39928	4.08462	17.28612	0.34901	4.08434	17.05091	0.35380	4.08419	16.97883	0.35529
0.75963	2.31644	4.04483	16.95813	0.35229	4.04458	16.73528	0.35696	4.04443	16.66216	0.35851
0.81199	2.23154	3.95964	16.49323	0.35459	3.95942	16.28068	0.35920	3.95929	16.21292	0.36069
0.83724	2.19440	3.90077	16.23405	0.35490	3.90056	16.02483	0.35951	3.90044	15.95891	0.36099

Table 3. Compactness ratio, u ($\equiv M/R$), and the fractional moment of inertia, Q ($\equiv I_{\text{core}}/I_{\text{total}}$), for different values of the ratio of pressure to energy-density, (P_0/E_0) , at the centre for the models presented in Table 2. For each value of (P_0/E_0) , the compactness ratio of homogeneous density sphere, u_h , is shown in column 2. Various parameters are obtained by assigning a fiduciary value of $E_b = 2.7 \times 10^{14} \text{ g cm}^{-3}$ for an assigned value of the ratio of pressure to energy-density, $(P_b/E_b) = (P_b/E_b)_1 \simeq 1.0645 \times 10^{-2}$, at the core-envelope boundary. The superscripts a, b, and c which appear among various parameters represent the models corresponding to an envelope with $\Gamma_1 = 4/3, 5/3$, and 2 respectively. The slanted values correspond to the limiting case upto which the configurations remain pulsationally ‘stable’. It is seen that for an assigned value of (P_0/E_0) the inequality, $u \leq u_h$, is always satisfied (but not ‘appropriately’ satisfied, cf. the caption of Table 2) by all members of the sequence corresponding to an envelope with $\Gamma_1 = 4/3$, whereas it remains unsatisfied by various members in the stable (as well as unstable) branch of the sequences corresponding to an envelope with $\Gamma_1 = 5/3$ and 2 respectively. It follows from this table that the choice of P_b/E_b ($\simeq 1.0645 \times 10^{-2}$; in the present context, for example) can provide a suitable explanation only for the higher values of the glitch healing parameter Q in the range, $0.558 \leq Q \leq 0.948$ (in the present context, for example), on the basis of the starquake mechanism of glitch generation as shown in Fig.3.

(P_0/E_0)	u_h	u^a	u^b	u^c	Q^a	Q^b	Q^c
0.10603	0.14794	0.12862	0.14020	0.14389	0.55820	0.65183	0.68421
0.11977	0.16070	0.14250	0.15367	0.15725	0.60171	0.68740	0.71684
0.12544	0.16567	0.14789	0.15897	0.16241	0.61720	0.70036	0.72805
0.13235	0.17152	0.15435	0.16514	0.16860	0.63523	0.71436	0.74134
0.15071	0.18603	0.17027	0.18057	0.18390	0.67538	0.74645	0.77083
0.18604	0.21029	0.19699	0.20654	0.20959	0.73256	0.79226	0.81213
0.22012	0.23000	0.21889	0.22770	0.23056	0.77223	0.82325	0.84041
0.25219	0.24591	0.23655	0.24486	0.24756	0.80003	0.84534	0.86049
0.28047	0.25823	0.25025	0.25817	0.26065	0.81961	0.86085	0.87416
0.31322	0.27081	0.26427	0.27172	0.27416	0.83806	0.87524	0.88769
0.33333	0.27778	0.27209	0.27926	0.28153	0.84795	0.88286	0.89418
0.35897	0.28593	0.28113	0.28801	0.29029	0.85858	0.89113	0.90219
0.37791	0.29149	0.28730	0.29402	0.29613	0.86561	0.89685	0.90686
0.43583	0.30640	0.30371	0.30991	0.31193	0.88305	0.91052	0.91962
0.48898	0.31785	0.31612	0.32191	0.32381	0.89536	0.92014	0.92842
0.56150	0.33083	0.32982	0.33521	0.33697	0.90837	0.93055	0.93793
0.63427	0.34152	0.34045	0.34553	0.34713	0.91811	0.93842	0.94493
0.66738	0.34577	<i>0.34440</i>	<i>0.34926</i>	<i>0.35090</i>	<i>0.92180</i>	<i>0.94106</i>	<i>0.94765</i>
0.68401	0.34778	0.34613	0.35100	0.35253	0.92331	0.94251	0.94864
0.70503	0.35021	0.34817	0.35294	0.35452	0.92529	0.94399	0.95028
0.71465	0.35128	0.34901	0.35380	0.35529	0.92604	0.94480	0.95070
0.75963	0.35600	0.35229	0.35696	0.35851	0.92925	0.94739	0.95349
0.81199	0.36095	0.35459	0.35920	0.36069	0.93215	0.94997	0.95578
0.83724	0.36314	0.35490	0.35951	0.36099	0.93292	0.95075	0.95650

Table 4. Mass (M), size (R), compactness ratio ($u \equiv M/R$), and the ‘local’ value of adiabatic index at the centre, $(\Gamma_1)_0$, for different values of the ratio of central pressure to central energy-density, (P_0/E_0) , for the core-envelope models discussed in the text (step (4), section 3). Various parameters are obtained by assigning a fiduciary value of $E_b = 2.7 \times 10^{14}$ g cm $^{-3}$ and for an ‘appropriate’ value of the ratio of pressure to energy-density, $(P_b/E_b) = (P_b/E_b)_2 \simeq 4.694 \times 10^{-2}$, at the core-envelope boundary. The superscripts a, b, and c which appear among various parameters represent the models corresponding to an envelope with $\Gamma_1 = 4/3, 5/3$, and 2 respectively. The slanted values correspond to the limiting case upto which the configurations remain pulsationally stable. It is seen that the $M - R$ relation does provide the necessary and sufficient condition of dynamical stability for all of the sequences, since all of the sequences satisfy both of the inequalities, viz. $u_{\max} \leq 0.3406$ and $(\Gamma_1)_0 \leq 2.5946$, simultaneously at the maximum value of mass. Because all members of the sequences corresponding to an envelope with $\Gamma_1 = 4/3, 5/3$ and 2 fulfill the ‘compatibility criterion’, $u \leq u_h$ (where u_h represents the compactness ratio of homogeneous density sphere for the corresponding value of P_0/E_0), together with fulfilling the necessary and sufficient condition of dynamical stability provided by the $M - R$ relation, it follows, therefore, that the assigned value of $(P_b/E_b) = (P_b/E_b)_2 \simeq 4.694 \times 10^{-2}$ corresponds to the *minimum* value for which the ‘compatibility criterion’ is ‘appropriately’ satisfied by all the sequences corresponding to NS models with an envelope $\Gamma_1 = 4/3, 5/3$ and 2 respectively as discussed in step (4) of section 3.

(P_0/E_0)	$(\Gamma_1)_0$	(M^a/M_\odot)	R^a (km)	u^a	(M^b/M_\odot)	R^b (km)	u^b	(M^c/M_\odot)	R^c (km)	u^c
0.10052	10.9487	1.79122	43.32919	0.06106	1.55535	20.66582	0.11116	1.47601	17.50211	0.12456
0.11236	9.90023	1.87195	39.26268	0.07042	1.67909	20.40422	0.12154	1.61142	17.58182	0.13537
0.12029	9.31353	1.93294	37.11014	0.07693	1.76262	20.27094	0.12843	1.70131	17.65121	0.14236
0.12955	8.71910	2.00865	35.04138	0.084665	1.85989	20.15492	0.13630	1.80486	17.73130	0.15034
0.14549	7.87332	2.14512	32.33658	0.09798	2.02462	20.01554	0.14940	1.97821	17.88177	0.16340
0.15354	7.51305	2.21518	31.27768	0.10461	2.10582	19.97345	0.15572	2.06296	17.95627	0.16969
0.20061	5.98487	2.61355	27.42286	0.14077	2.54549	19.87280	0.18919	2.51677	18.35244	0.20255
0.23990	5.16877	2.91143	25.75275	0.16698	2.86158	19.87300	0.21268	2.83972	18.61125	0.22536
0.27901	4.58413	3.17036	24.69328	0.18963	3.13199	19.87624	0.23274	3.11471	18.80100	0.24469
0.34816	3.87220	3.54016	23.49470	0.22255	3.51403	19.84340	0.26156	3.50187	18.97877	0.27253
0.44840	3.23013	3.90788	22.35809	0.25816	3.89112	19.64414	0.29256	3.88312	18.97775	0.30222
0.48306	3.07012	3.99636	22.02864	0.26795	3.98169	19.54181	0.30094	3.97464	18.92270	0.31024
0.51773	2.93149	4.06762	21.71508	0.27667	4.05467	19.41360	0.30848	4.04842	18.83572	0.31746
0.54455	2.83637	4.11157	21.47901	0.28273	4.09975	19.30104	0.31373	4.09402	18.74922	0.32251
0.58709	2.70330	4.16243	21.10649	0.29128	4.15213	19.09782	0.32112	4.14711	18.58635	0.32956
0.63150	2.58354	4.19170	20.70981	0.29895	4.18272	18.84735	0.32778	4.17831	18.37295	0.33589
0.66866	2.49552	4.19788	20.36982	0.30438	4.18981	18.61628	0.33242	4.18584	18.16228	0.34040
0.68296	2.46421	4.19565	20.23663	0.30623	4.18789	18.51726	0.33404	4.18408	18.07316	0.34194
0.69900	2.43062	4.19032	20.08121	0.30820	4.18289	18.40185	0.33573	4.17923	17.96912	0.34352
0.72302	2.38309	4.17593	19.84795	0.31076	4.16896	18.22159	0.33793	4.16552	17.79888	0.34567
0.74010	2.35117	4.16090	19.67543	0.312351	4.15423	18.08144	0.33934	4.15094	17.66827	0.34700
0.77503	2.29027	4.11752	19.30611	0.31501	4.11141	17.77494	0.34164	4.10839	17.38013	0.34914
0.80605	2.24061	4.06269	18.95854	0.31651	4.05700	17.47310	0.34294	4.05419	17.08740	0.35044
0.83972	2.19088	3.98260	18.54954	0.31711	3.97730	17.10352	0.34347	3.97469	16.72970	0.35091

Table 5. Compactness ratio, u ($\equiv M/R$), and the fractional moment of inertia, Q ($\equiv I_{\text{core}}/I_{\text{total}}$), for different values of the ratio of pressure to energy-density, (P_0/E_0) , at the centre for the models presented in Table 4. For each value of (P_0/E_0) , the compactness ratio of homogeneous density sphere, u_h , is shown in column 2. Various parameters are obtained by assigning a fiduciary value of $E_b = 2.7 \times 10^{14} \text{ g cm}^{-3}$ and for an ‘appropriate’ value of the ratio of pressure to energy-density, $(P_b/E_b) = (P_b/E_b)_2 \simeq 4.694 \times 10^{-2}$, at the core-envelope boundary. The superscripts a, b, and c which appear among various parameters represent the models corresponding to an envelope with $\Gamma_1 = 4/3, 5/3$, and 2 respectively. The slanted values correspond to the limiting case upto which the configurations remain pulsationally stable. It is seen that for an assigned value of (P_0/E_0) , the inequality, $u \leq u_h$, is ‘appropriately’ satisfied by all members of the sequences corresponding to an envelope with $\Gamma_1 = 4/3, 5/3$ and 2 respectively. It follows from this table that the ‘appropriate’ choice of P_b/E_b ($\simeq 4.694 \times 10^{-2}$; in the present context, for example) can provide a suitable explanation for both (the higher as well as lower) values of the glitch healing parameter Q in the range, $0.016 \leq Q \leq 0.779$ (in the present context, for example), on the basis of the starquake mechanism of glitch generation as shown in Fig.5.

(P_0/E_0)	u_h	u^a	u^b	u^c	Q^a	Q^b	Q^c
0.10052	0.14253	0.06106	0.11116	0.12456	0.01548	0.06873	0.09775
0.11236	0.15394	0.07042	0.12154	0.13537	0.02739	0.09920	0.13475
0.12029	0.16116	0.07693	0.12843	0.14236	0.03739	0.12071	0.15969
0.12955	0.16918	0.08466	0.13630	0.15034	0.05089	0.14626	0.18860
0.14549	0.18205	0.09798	0.14940	0.16340	0.07777	0.19020	0.23645
0.15354	0.18814	0.10461	0.15572	0.16969	0.09261	0.21182	0.25950
0.20061	0.21911	0.14077	0.18919	0.20255	0.18555	0.32652	0.37684
0.23990	0.24008	0.16698	0.21268	0.22536	0.26028	0.40470	0.45366
0.27901	0.25763	0.18963	0.23274	0.24469	0.32671	0.46877	0.51517
0.34816	0.28259	0.22255	0.26156	0.27253	0.42326	0.55590	0.59803
0.44840	0.30929	0.25816	0.29256	0.30222	0.52531	0.64342	0.67967
0.48306	0.31666	0.26795	0.30094	0.31024	0.55283	0.66607	0.70070
0.51773	0.32332	0.27667	0.30848	0.31746	0.57715	0.68625	0.71944
0.54455	0.32803	0.28273	0.31373	0.32251	0.59401	0.70020	0.73250
0.58709	0.33482	0.29128	0.32112	0.32956	0.61777	0.71982	0.75062
0.63150	0.34115	0.29895	0.32778	0.33589	0.63925	0.73770	0.76712
0.66866	0.34593	<i>0.30438</i>	<i>0.33242</i>	<i>0.34040</i>	<i>0.65474</i>	<i>0.75034</i>	<i>0.77916</i>
0.68296	0.34766	0.30623	0.33404	0.34194	0.66008	0.75491	0.78336
0.69900	0.34952	0.30820	0.33573	0.34352	0.66592	0.75976	0.78778
0.72302	0.35220	0.31076	0.33793	0.34567	0.67364	0.76625	0.79403
0.74010	0.35401	0.31235	0.33934	0.34700	0.67868	0.77068	0.79815
0.77503	0.35751	0.31501	0.34164	0.34914	0.68772	0.77855	0.80543
0.80605	0.36041	0.31651	0.34294	0.35044	0.69398	0.78427	0.81111
0.83972	0.36336	0.31711	0.34347	0.35091	0.69887	0.78917	0.81587